The tetravalent organic cation spermine causes the gating of the IRK1 channel expressed in murine fibroblast cells

Keiko Ishihara*, Masayasu Hiraoka† and Rikuo Ochi

Department of Physiology, Juntendo University School of Medicine, 2-1-1, Hongo, Bunkyo-ku, Tokyo 113 and †Department of Cardiovascular Diseases, Medical Research Institute, Tokyo Medical and Dental University, 1-5-45 Yushima, Bunkyo-ku, Tokyo 113, Japan

1. The activation kinetics of the IRK1 channel stably expressed in L cells (a murine fibroblast cell line) were studied under the whole-cell voltage clamp. Without polyamines or Mg^{2+} in the pipettes, inward currents showed an exponential activation on hyperpolarization. The steep inward rectification of the currents around the reversal potential (E_{rev}) could be described by the open–close transition of the channel with first-order kinetics.

2. When the tetravalent organic cation spermine (Spm) was added in the pipettes, the activation kinetics changed; this was explicable by the increase in the closing rate constant. The activation of the currents observed without Spm or Mg^{2+} in the pipettes was ascribed to the unblocking of the 'endogenous-Spm block'.

3. In the presence of the divalent cation putrescine (Put) or of Mg^{2+} in the pipettes, a different non-conductive state suppressed the outward currents on depolarization; the channels instantaneously changed to the open state on repolarization. As the depolarization was prolonged, this non-conductive state was replaced by the non-conductive state that shows an exponential activation on repolarization. This phenomenon was attributed to the redistribution of the channels from the Put- or Mg^{2+}-blocked state to the 'endogenous Spm-blocked state' during depolarization.

4. In the presence of the trivalent cation spermidine (Spd) in the pipettes, two different non-conductive states occurred, showing a faster and a slower activation on repolarization. The rectification around E_{rev} was mainly due to the non-conductive state showing a faster activation, which appeared to be the Spd-blocked state. During depolarization, redistribution of the channels to the 'endogenous Spm-blocked state' also occurred.

5. In the presence of Spd, Put or Mg^{2+} in the pipettes, the voltage dependence of the activation time constant reflecting the unblocking of the 'endogenous Spm' was shifted in the hyperpolarizing direction.

6. Our results suggest that the 'intrinsic gating' that shows the time-dependent activation on repolarization, and that is responsible for the inward rectification around E_{rev}, reflects the blocking kinetics of the tetravalent Spm.

Inward rectifier K^+ channels expressed in a variety of cell types rectify strongly, and show a time- and voltage-dependent activation following an instantaneous current jump on hyperpolarization. The steep inward rectification around the reversal potential (E_{rev}), and the time-dependent property of the currents have been described by the open–close transition of the activation gate, which apparently depends on the extracellular K^+ concentration ($[K^+]_o$) (Hagiwara, Miyazaki & Rosenthal, 1976; Leech & Stanfield, 1981; Kurachi, 1985). As the mechanism accounting for this inward rectification, the block of the channel by an internal molecule has been proposed (Hagiwara & Takahashi, 1974; Hille & Schwarz, 1978). The intracellular cations Mg^{2+} (Horie, Irisawa & Noma, 1987;

* To whom correspondence should be addressed at the Department of Physiology, Saga Medical School, 5-1-1 Nabeshima, Saga 849, Japan.

Matsuda, Saigusa & Irisawa, 1987; Vandenberg, 1987), Ca^{2+} (Mazzanti & DiFrancesco, 1989; Matsuda & Cruz, 1993) and Na^{+} (Matsuda, 1993) have been shown to block inward rectifier K^{+} channels at the single channel level. Of these, Mg^{2+} showed the most potent blocking effect (Matsuda & Cruz, 1993). However, the activation kinetics (the major determinant of the inward rectification around E_{rev}) were shown to be different from the fast kinetics of the Mg^{2+} block (Ishihara, Mitsuiye, Noma & Takano, 1989; Silver & DeCoursey, 1990). Therefore, the inward rectification has been considered to be an intrinsic property of the channel protein modulated by K^{+} binding to the regulatory binding sites of the channel (Ciani, Krasne, Miyazaki & Hagiwara, 1978; Carmeliet, 1982; Pennefather, Oliva & Mulrine, 1992; Pennefather & DeCoursey, 1994).

Recently, genes encoding the inward rectifier K^{+} channels have been cloned (for a review, see Kubo, 1994). One of the cloned channels, the IRK1 channel (Kubo, Baldwin, Jan & Jan, 1993), possesses a gating mechanism similar to that characterized in the native channels (Stanfield *et al.* 1994*a*; Wible, Taglialatela, Ficker & Brown, 1994; Ishihara & Hiraoka, 1994). Extensive studies on the cloned channels have revealed that the block of the channels by intracellular polyamines (organic cations) is responsible for the steep rectification of the IRK1 channel and its homologue the HIRK1 channel (Makhina, Kelly, Lopatin, Mercer & Nichols, 1994; Perier, Radeke & Vandenberg, 1994) expressed in *Xenopus* oocytes (Lopatin, Makhina & Nichols, 1994; Ficker, Taglialatela, Wible, Henley & Brown, 1994; Fakler *et al.* 1994; Fakler, Brandle, Glowatzki, Weidemann, Zenner & Ruppersberg, 1995). Ficker *et al.* (1994) showed further that block of the channel by the tri- and tetravalent polyamines spermidine (Spd) and spermine (Spm) is responsible for the time-dependent activation of the inward currents. However, polyamine-independent activation of the current has been shown by Fakler *et al.* (1994, 1995) in the IRK1 channel expressed in *Xenopus* oocytes, which was slowed down in the presence of internal Mg^{2+}, as has been shown for the IRK1 channel expressed in the murine erythroleukaemia cell line (Stanfield *et al.* 1994*b*).

In the present study, we asked whether the time-dependent activation of the IRK1 channel reflects the kinetics of the polyamine block. We established cell lines stably expressing the IRK1 gene, and recorded whole-cell currents by the patch clamp method in a condition in which endogenous polyamines remained in the intracellular milieu. We added in the pipettes three different polyamines, Spm, Spd or putrescine (Put), to restore the polyamines in the cells, and examined the effects on the activation kinetics of the IRK1 channel. Our results strongly suggested that the activation phase of the inward currents reflects the unblocking of the endogenous Spm, which remained in the cells without being completely diffused out under the whole-cell clamp conditions. Our data suggested further that Spd also contributes to the rectification around E_{rev} in a physiological condition. Although Put, the divalent polyamine, blocked the channels on depolarization, the Put block was replaced by the endogenous Spm block in a time-dependent manner, similar to the block by Mg^{2+} (Ishihara *et al.* 1989).

METHODS

Establishment of L cell clones expressing the IRK1 gene

The cDNA of the IRK1 gene (Kubo *et al.* 1993) was subcloned into the expression vector pCXN2 (Niwa, Yamamura & Miyazaki, 1991) and transfected to L cells (a mouse fibroblast cell line) by electroporation (Yanagi, Hu, Seya & Yoshikura, 1994). L cells were obtained from the Department of Enteroviruses, National Institute of Health, Japan. The clones functionally expressing the IRK1 gene were selected from the G418 (500 $\mu g\ ml^{-1}$)-resistant clones using the electrophysiological method. The IRK1-expressing L cells thus obtained were grown in Dulbecco's modified Eagle's medium supplemented with 10% fetal bovine serum.

Solutions

The Mg^{2+}-free external solution contained (mM): 140 NaCl, 5·4 KCl, 1·8 $CaCl_2$, 0·33 NaH_2PO_4 and 5 Hepes–NaOH (pH 7·4). Except for the data in Fig. 6, all data were collected at 5·4 mM K^{+}_{o}. When $[K^{+}]_o$ was increased to 15·4 mM to obtain the data in Fig. 6, isomolar NaCl was replaced with KCl. The Mg^{2+}-free–polyamine-free pipette solution contained (mM): 20 KCl, 90 potassium aspartate, 10 KH_2PO_4, 5 EDTA, 1·9 K_2ATP and 5 Hepes–KOH (pH 7·2). Assuming that the deionized water used to make the solution contained 10 μM Ca^{2+} and Mg^{2+}, the concentration of free divalent cations is estimated to be less than 10^{-8} M using the formula developed by Fabiato & Fabiato (1979). Spm, Spd, or Put (Sigma) were added to the Mg^{2+}-free–polyamine-free pipette solution at 500 μM, which is close to the total concentration of Spm or Spd in animal cells (0·88–1·57 mM; Watanabe, Kusama-Eguchi, Kobayashi & Igarashi, 1991). Polyamines bind to ATP and intracellular macromolecules, such as RNA or DNA (Watanabe *et al.* 1991). We added polyamines to the pipette solution containing a physiological concentration of ATP (2–3 mM; Watanabe *et al.* 1991) to keep ATP from diffusing out of the intracellular milieu. Therefore, the intracellular concentrations of free polyamines in our experiments are expected to be similar to those under physiological conditions (Spm and Spd, 15–200 μM; Watanabe *et al.* 1991). The Mg^{2+} pipette solution contained 7·9 mM $MgCl_2$ in addition to the Mg^{2+}-free–polyamine-free solution. The free Mg^{2+} concentration was estimated to be 1·14 mM. The total K^{+} concentration in the pipette solutions was ~150 mM.

Measurements of the IRK1-expressed currents and data analysis

Before the experiments, cells were suspended in phosphate-buffered saline containing 0·5 mM EDTA so that they were spherical in shape, with an input capacitance of 26·9 ± 6·6 pF (mean ± S.D., $n = 39$). Membrane currents were measured under whole-cell patch clamp using an EPC-7 amplifier (List Electronic). Pipette resistance was less than 2 MΩ when filled with the pipette solutions. The junction potentials in the pipettes were measured to be about −10 mV in relation to the external solution, and all membrane potentials were corrected for this value. Voltage

stimulation and data acquisition were performed by the pCLAMP software (v. 6.02, Axon Instruments) on a 486 DOS/V computer (Compaq Prolinea 4/33) through the Labmaster TL-1 interface (Axon Instruments). All experiments were conducted at room temperature (21–23 °C). Data were analysed using pCLAMP and SigmaPlot software (v. 4.16; Jandel Corp., San Rafael, CA, USA). The horizontal dashed lines superimposed on current traces indicate the zero current level. The time-dependent current amplitude was measured by extrapolating the fitted exponential curves to the onset of the voltage change. The onset was set at the time when the amplitude of the capacitive transient decreased to 1/e.

RESULTS

Expression of the IRK1 channel in the L cell line

The membrane conductance of the parental L cells was negligible at various $[K^+]_o$ levels (Fig. 1*A*, upper panel). We derived the L cell lines stably expressing the IRK1 gene by DNA transfection (Fig. 1*A*, lower panel). The conductance of the L cells functionally expressing the IRK1 gene showed a steep inward rectification with the maximum value of $1{\cdot}2 \pm 0{\cdot}5$ μS nF^{-1} ($n = 13$) at 5·4 mM K_o^+. E_{rev} of the expressed currents determined at 5·4 mM K_o^+ was

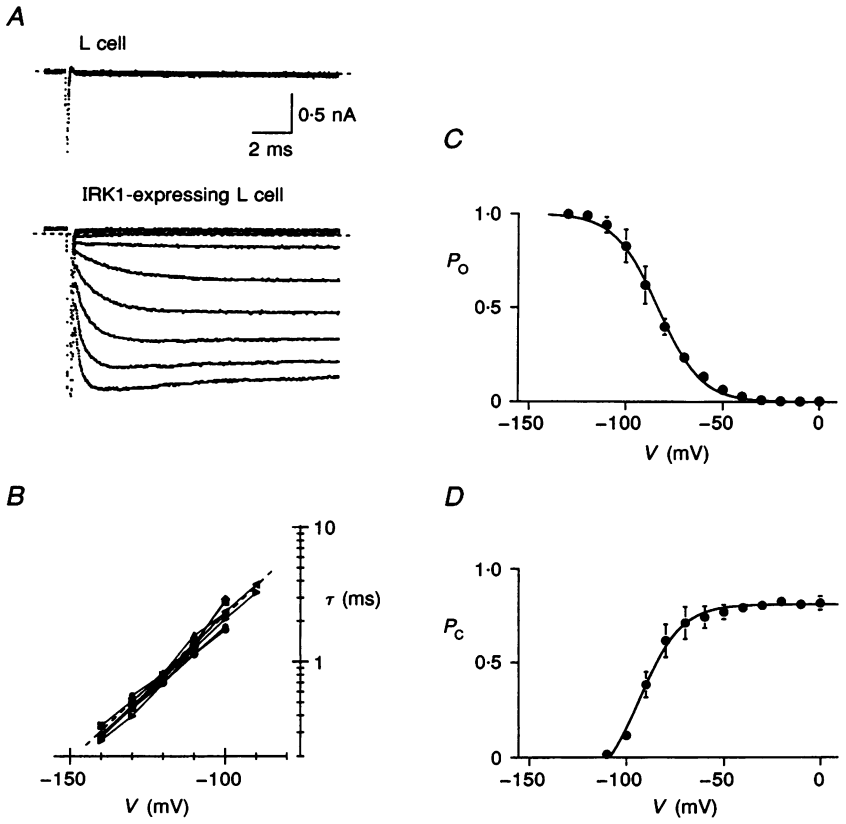

Figure 1. Current changes of the IRK1 channel recorded using the Mg^{2+}-free–polyamine-free pipettes

A, expression of the IRK1 channel. Upper panel, currents recorded from the parental L cell. Lower panel, currents from the IRK1 gene-expressing L cell at 20 min after starting the experiment. In both records, the potential range for the voltage steps was from −140 mV (the bottom) to −60 mV (the top) in 10 mV increments. Holding potential, −10 mV. *B*, relationship between the time constant (τ) of the inward currents and the membrane potential (V). The time constants were fitted to τ (ms) $= k \exp(V/s)$ using $k = 317{\cdot}8$ ms and $s = 20{\cdot}2$ mV (the dashed line); $n = 7$. *C*, voltage dependence of P_O. The normalized chord conductance obtained at the end of 500 ms voltage steps applied from −130 mV is plotted as P_O. Data were obtained at least 5 min after starting experiments. The error bars indicate the standard deviation ($n = 5$). The fitted curve indicates the Boltzmann expression:

$$P_O = \{1 + \exp[(V - (-83{\cdot}6))/-11{\cdot}1]\}^{-1}.$$

D, voltage dependence of P_C obtained at the end of 500 ms voltage steps applied from −130 mV. Tail currents at −130 mV following voltage steps were fitted by single exponential curves, and the amplitude of the time-dependent component relative to the maximum level of the inward current at −130 mV is plotted as P_C against the preceding potential. The error bars indicate the standard deviation ($n = 5$). The fitted curve indicates:

$$P_C = 0{\cdot}81 - \{1 + \exp[(V - (-93{\cdot}1))/-10{\cdot}6]\}^{-1}.$$

$-81{\cdot}1 \pm 0{\cdot}8$ mV ($n = 10$), and shifted to $-53{\cdot}8 \pm 0{\cdot}9$ mV ($n = 5$) by increasing $[K^+]_o$ to 15·4 mM. These values were about 4 mV less negative than the K^+ equilibrium potential (E_K) estimated from the Nernst equation assuming the intracellular K^+ concentration to be 150 mM. However, the shift of E_{rev} corresponds to a 59·3 mV change per tenfold change in $[K^+]_o$, indicating that the expressed channels are selectively permeable to K^+.

Activation kinetics of the IRK1 channel in the absence of Mg^{2+} and polyamines in the pipettes

When the whole-cell currents were recorded from the IRK1-expressing L cells using the pipettes containing no Mg^{2+} and polyamines, they stably showed a steep inward rectification around E_{rev}. Upon membrane hyperpolarization from a depolarized holding potential, inward currents showed a single exponential increase (Fig. 1*A*; Stanfield *et al.* 1994*a*). The time constants did not significantly alter even during experiments that lasted longer than 1 h, and they decreased e-fold for a 20·2 mV hyperpolarization (Fig. 1*B*). The single exponential increase of the inward currents has been attributed to the transition of the channels from the single non-conductive state (C) that is independent of the Mg^{2+}-blocked state, to the open state (O) (Ishihara *et al.* 1989; Silver & DeCoursey, 1990; Stanfield *et al.* 1994*a*). The simple scheme for this gating is:

$$C \underset{\beta}{\overset{\alpha}{\rightleftharpoons}} O, \qquad (1)$$

where α and β are the voltage-dependent rate constants (s^{-1}). Figure 1*C* shows the voltage dependence of the open probability of the channel (P_O) obtained from the normalized chord conductance at the end of 500 ms voltage steps. The probability of the channel being in the state C (P_C) at the end of voltage steps was obtained from the amplitude of the time-dependent inward currents at -130 mV following voltage steps (Fig. 1*D*). The maximum P_C did not reach 1·0, but saturated around 0·8 even at positive potentials where P_O was negligible. Similar descriptions have been made for the native channels (Hagiwara *et al.* 1976; Leech & Stanfield, 1981; Silver & DeCoursey, 1990). This implies that an additional non-conductive state(s) contributes to the rectification. However, the sum of P_O and P_C was nearly 1·0 at potentials negative to -70 mV, indicating that the steep rectification of the currents can be described with the above kinetic model at this potential range. Therefore, we estimated the voltage dependence of α and β at large negative potentials between -90 and -140 mV using the experimental results (Fig. 2*A*).

Recently, the activation kinetics were proposed to be caused by the release of polyamine block of the channels (Lopatin *et al.* 1994; Ficker *et al.* 1994). In this case, the state C is the blocked state of the channel, and the kinetics should be expressed as:

$$C \underset{[T]\beta_T}{\overset{\alpha}{\rightleftharpoons}} O, \qquad (2)$$

where [T] is the intracellular concentration of the blocking molecule (M) and β_T is the second-order rate constant ($M^{-1}\,s^{-1}$). The apparent blocking rate constant β shown in Fig. 2*A* should correspond to $[T]\beta_T$. If the influence of the membrane potential on the local concentration of the blocking molecule near the channel pore can be ignored, β should change according to the change in [T] as shown by the dashed curves in Fig. 2*A*. The changes in the time constant and P_O expected from the changes in β are shown in Fig. 2*B* and *C*, respectively. The voltage dependence of P_C in Fig. 1*D* should also shift in the hyperpolarizing direction in parallel with the shift of P_O. In the following

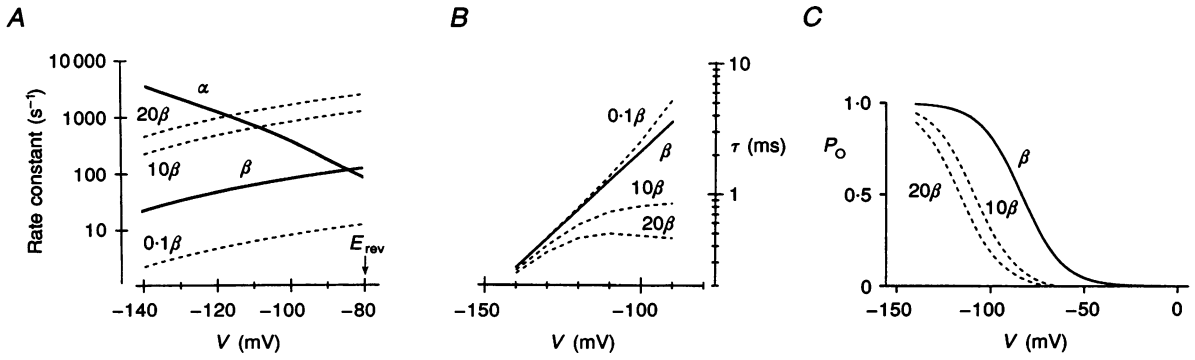

Figure 2. Opening (α) and closing (β) rate constants obtained with the Mg^{2+}-free–polyamine free pipettes

A, voltage dependence of α and β were calculated using the equations $\tau = (\alpha + \beta)^{-1}$ and $P_O = \alpha(\alpha + \beta)^{-1}$ from the experimental results in Fig. 1*B* and *C* (continuous curves). Changes in β to the levels of 20, 10 and 0·1 times are indicated by the dashed curves. *B*, changes in the time constant expected from the changes in β (dashed curves). The continuous line represents the data in Fig. 1*B*. *C*, changes in P_O expected from the increase in β (dashed curves). The continuous curve represents the data in Fig. 1*C*.

experiments, we added different kinds of polyamines to the Mg^{2+}-free–polyamine-free solution, and examined the effects on the time-dependent activation of the IRK1 channel.

Effects of Spm on the activation kinetics

We first tested the effects of Spm, a tetravalent polyamine, on the currents through the IRK1 channel. Figure 3*A* shows the currents in response to hyperpolarization. The inward currents showed a time-dependent activation, which could be approximated by a single exponential curve as shown in Fig. 3*A b*. Figure 3*B* shows the relationship between the time constant and the membrane potential in the hyperpolarization. The time constants were smaller than those obtained using the Mg^{2+}-free–polyamine-free pipettes at potentials positive to −110 mV, thereby reducing their voltage dependence. In some cases, the time constant at −100 mV was even smaller than that at

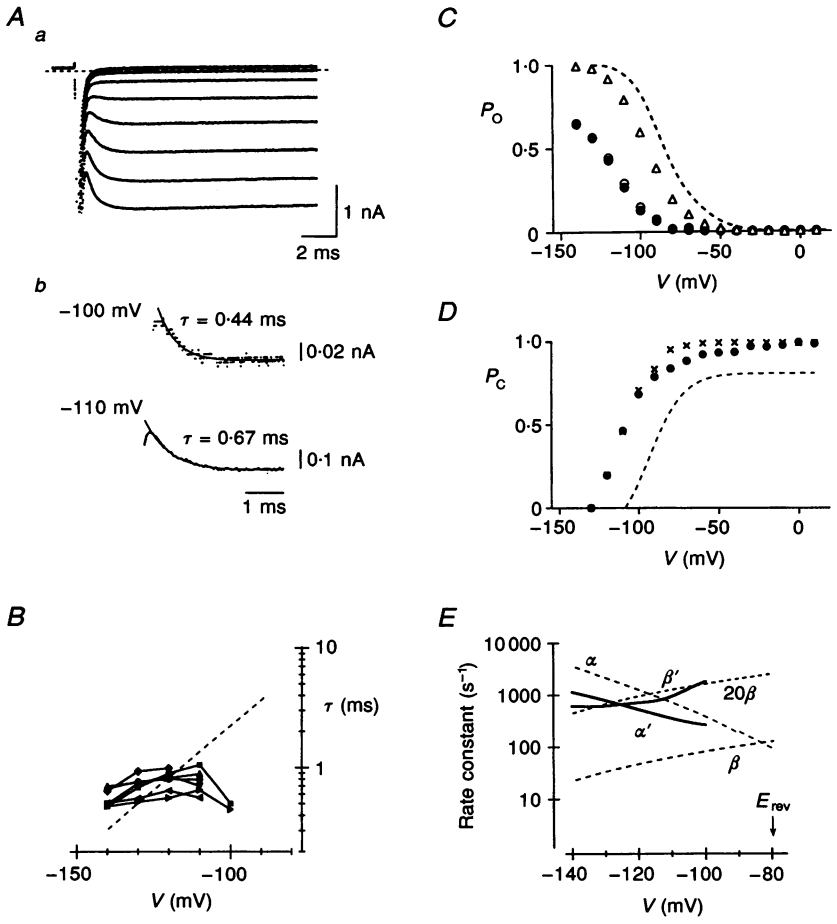

Figure 3. Effects of the tetravalent cation Spm on the activation kinetics

A, currents recorded using the Spm pipette. *a*, superimposed currents were elicited by voltage steps ranging from −140 mV (the bottom) to −60 mV (the top) in 10 mV increments. Holding potential, −10 mV. *b*, enlargement of the currents at −100 and −110 mV shown in *a*. Each current is fitted by a single exponential curve with the time constant indicated. *B*, relationship between the time constant of the inward currents and the membrane potential ($n = 6$). Data were obtained from the currents recorded as in Fig. 3*A*, at least 15 min after starting experiments. The dashed line represents data in Fig. 1*B*. *C*, voltage dependence of P_O obtained at 1 min (△), 15 min (○) and 21 min (●) after making the whole-cell patch. The chord conductance is plotted, which was calculated from the current levels at the end of 500 ms voltage steps applied from −130 mV, and normalized with the maximum value at 1 min. The dashed curve represents the data in Fig. 1*C*. *D*, voltage dependence of P_C at the end of 500 ms voltage steps applied from −130 mV (●). Values were obtained as described in Fig. 1*D*. Time constants of the inward currents at −130 mV used to obtain the data were not affected by the preceding potential ($0{\cdot}79 \pm 0{\cdot}05$ ms, $n = 14$). P_O at the end of voltage steps was obtained by normalizing the chord conductance with the maximum value at −130 mV, and the value $1 - P_O$ is also plotted (×). The dashed curve represents the data in Fig. 1*D*. *E*, estimation of the rate constants in the presence of Spm based on the two-states model. The opening (α') and the closing (β') rate constants were calculated using τ in *B* (mean value was obtained at each membrane potential), and P_O at 15 min in *C*. α, β and 20β in Fig. 2*A* are indicated by the dashed curves.

−110 mV as shown in Fig. 3*A b*. The change in the time constant caused by Spm was similar to what was expected from the increase in the rate constant β (Fig. 2*B*).

When the pipettes contained Spm, the inward rectification of the currents became more pronounced several minutes after starting the experiment. Figure 3*C* demonstrates the chronological change of the voltage dependence of P_O during the experiment. Spm in the pipette not only shifted the relationship in the hyperpolarizing direction, but also reduced the maximum conductance ($n = 5$). The voltage dependence of P_C determined from the relative amplitude of the time-dependent inward currents was also shifted in the hyperpolarizing direction by Spm (Fig. 3*D*), and the relationship agreed with the voltage dependence of the value $1 - P_O$ obtained in the same experiment. These findings indicate that the strong inward rectification of the currents in the presence of Spm is due to the voltage-dependent increase of the single non-conductive state C. The rate constants in the kinetic scheme (1) were calculated using the experimental results obtained in the presence of Spm, and are plotted as α' and β' in Fig. 3*E*. The rate constant β' was comparable with 20 times the value of β obtained with the Mg^{2+}-free–polyamine-free pipettes. The rate constant α' was shifted in the hyperpolarizing direction by 10–20 mV compared with α. If the shift of α was caused by the decrease in the negative surface potential by screening the fixed negative charges on the membrane surface or in the channel protein, a similar shift may have occurred for β'. Considering this shift, β' is still larger than β by about 10 times at each membrane

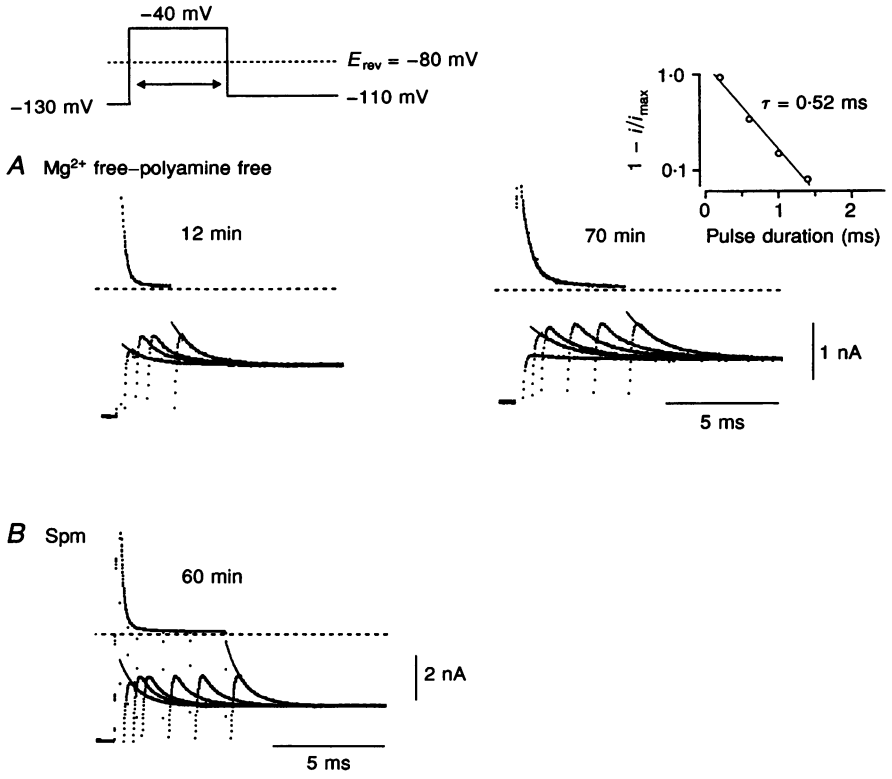

Figure 4. Deactivation time course revealed by the envelope test in the absence (*A*) or presence (*B*) of Spm in the pipettes

Time course of the deactivation was examined using the envelope test. The membrane potential was depolarized from −130 mV, the potential that maximally activates the channel at 5·4 mM K_O^+, to −40 mV for various periods of time, and repolarized to −110 mV. Shown superimposed are the decay of the outward currents during depolarization and the time-dependent activation of the inward currents on repolarization, recorded with different pulse durations. *A*, currents recorded using the Mg^{2+}-free–polyamine-free pipette at 12 min (left) and 70 min (right) after starting the experiment. Durations of depolarizing pulses were 0·2, 0·7, 1·2 and 2·45 ms (left), and 0·2, 0·6, 1, 2·2, 3·4 and 5 ms (right). Single exponential curves with the time constants of 1·2 ms (left) and 1·6 ms (right) are fitted to the inward currents. Inset, to show the time course of the envelope, the amplitude of the time-dependent components (i) was normalized with its maximum value (i_{max}), and the value $1 - i/i_{max}$ is plotted against the duration of the preceding depolarization. *B*, currents recorded using the Spm pipette at 60 min after starting the experiment. Durations of depolarizing pulses were 0·2, 0·6, 1, 2·2, 3·4 and 5 ms. The time constant of the fitted exponential curves is 0·8 ms.

potential. This finding strongly suggests that β is the blocking rate constant of the endogenous Spm, and the addition of Spm in the pipettes increased the surface concentration of Spm by about 10–20 times. The time-dependent activation of the inward currents constantly observed using the Mg^{2+}-free–polyamine-free pipettes (Fig. 1*A*) appeared to reflect the unblocking of the endogenous Spm block.

Effects of Spm on the deactivation kinetics

We also examined the effects of Spm on the deactivation process, the transition of the channels from the state O to the state C, which occurs on depolarization (Fig. 4). The time course of the deactivation was examined using the envelope test. After the channels were maximally distributed to the state O at −130 mV, the depolarizing pulse was given to −40 mV for various periods of time, and the proportion of the channels changed to the state C was estimated from the amplitude of the time-dependent inward current observed on the following repolarization. Families of currents in Fig. 4*A* are the representative currents recorded using the Mg^{2+}-free–polyamine-free pipette at 12 and 70 min after starting the experiment. The amplitude of the time-dependent component in the inward current on repolarization increased by extending the preceding depolarization, due to the time-dependent increase of the channels in the state C. At 12 min, the time-dependent component developed in the inward current with 0·2 ms depolarization (the first pulse), and saturated with 0·7 ms depolarization (the second pulse), indicating the fast transition of the channels from state O to state C. The transition became gradually slower during the experiment. At 70 min, the time-dependent inward current following the first 0·2 ms pulse became obviously smaller than that at 12 min, and the time course of the envelope could be approximated with a single exponential with the time constant of 0·52 ms (Fig. 4*A*, inset). The time constants obtained using the depolarizing pulses at −60 and −20 mV were 1·02 and 0·38 ms, respectively, indicating that the deactivation kinetics are voltage dependent. The slowing down of the deactivation during the course of the experiment is compatible with the idea that the voltage-dependent kinetics of the deactivation are caused by the soluble component in the cell (Matsuda, 1988; Lopatin *et al.* 1994; Ficker *et al.* 1994). Figure 4*B* shows the envelope test performed in the presence of Spm in the pipette. Even at 60 min after making the whole-cell patch, a large time-dependent component was observed in the inward current following the first 0·2 ms pulse. In the presence of Spm, the time course of the deactivation was so fast that the time constant could not be determined by the envelope test ($n = 6$). These findings support further the idea that Spm is the blocking molecule of the channel causing the non-conductive state C.

Non-conductive state that opens instantaneously on hyperpolarization in the presence of Put

The divalent polyamine Put in the pipettes apparently slowed the deactivation process on depolarization, in contrast to the effect of Spm. Currents in Fig. 5*A* were recorded by first hyperpolarizing the membrane potential from the holding potential of −40 mV to −130 mV to put the channels maximally in the state O, and depolarizing it back to −40 mV for various periods of time, and then hyperpolarizing it again to −130 mV. On hyperpolarization from the holding potential of −40 mV, a time-dependent increase of the inward current was observed, while the hyperpolarization following a short depolarization evoked a marked instantaneous current jump. Prolongation of the depolarization gradually increased the amplitude of the time-dependent component in the inward current on repolarization. Each time-dependent inward current could be fitted by a single exponential with the same time constant irrespective of the duration of the preceding depolarization as shown by the superimposed curves, indicating that the channels in the discrete state C increased slowly during depolarization. The upper panel of Fig. 5*B* shows the time course of the increase of P_C obtained from the amplitude of the time-dependent current on repolarization. As the membrane potential in the depolarization was made more positive (−60, −40 and −20 mV), the increase of P_C became significantly slower. The plot shown in the middle panel of Fig. 5*B* indicates the time course of the decrease of P_O during depolarization. P_O was reduced instantaneously on depolarization, and decreased further in a time-dependent manner. The degree of the instantaneous reduction of P_O (indicated by the arrows) was larger at more depolarized potentials. The value $1 - P_O - P_C$ shown in the lower panel represents the probability of the channel being in the non-conductive state that opens virtually instantaneously on hyperpolarization. The probability of the channel being in this additional non-conductive state increased rapidly on depolarization, and decreased slowly during depolarization. The rate of the decrease became slower as the membrane potential in the depolarization was made more positive. This non-conductive state that appeared in the presence of Put can be inferred to be the Put-blocked state. The virtually instantaneous unblocking of the Put-blocked channels appeared to be similar to the unblocking of Mg^{2+} shown in the native inward rectifier K^+ channel (Ishihara *et al.* 1989). The plots in Fig. 5*B* strongly suggest that a large fraction of the channels were first blocked by Put on depolarization, which instantaneously suppressed the outward currents, and were then reoccupied by the endogenous Spm, which produced the time-dependent decrease of P_O.

The same phenomenon, the slowing down of the O to C transition during depolarization, was observed in the presence of intracellular Mg^{2+} in the native channel

(Ishihara *et al.* 1989; Cohen, DiFrancesco, Mulrine & Pennefather, 1989) and in the IRK1 channel (Stanfield *et al.* 1994*a*). Using the pipettes containing 1 mM free Mg^{2+}, we confirmed that the increase of the channels in the state C also becomes slower as the depolarization becomes larger (Fig. 6). In this case, the instantaneous increases of P_C and $1 - P_O - P_C$ were observed on depolarization, suggesting that the channels can directly change to either the endogenous-Spm-blocked state or the Mg^{2+}-blocked state. In Fig. 7 we show the voltage dependence of P_C, P_O and the value $1 - P_O - P_C$ in the presence of Put or Mg^{2+} in the pipettes to characterize this phenomenon further.

Voltage dependence of the distribution of the non-conductive states in the presence of Put or Mg^{2+}

Figure 7 shows the voltage dependence of P_C, P_O and the value $1 - P_O - P_C$ obtained using pipettes containing Put or Mg^{2+}. The time-dependent changes in the relationships were obtained by applying three different durations of

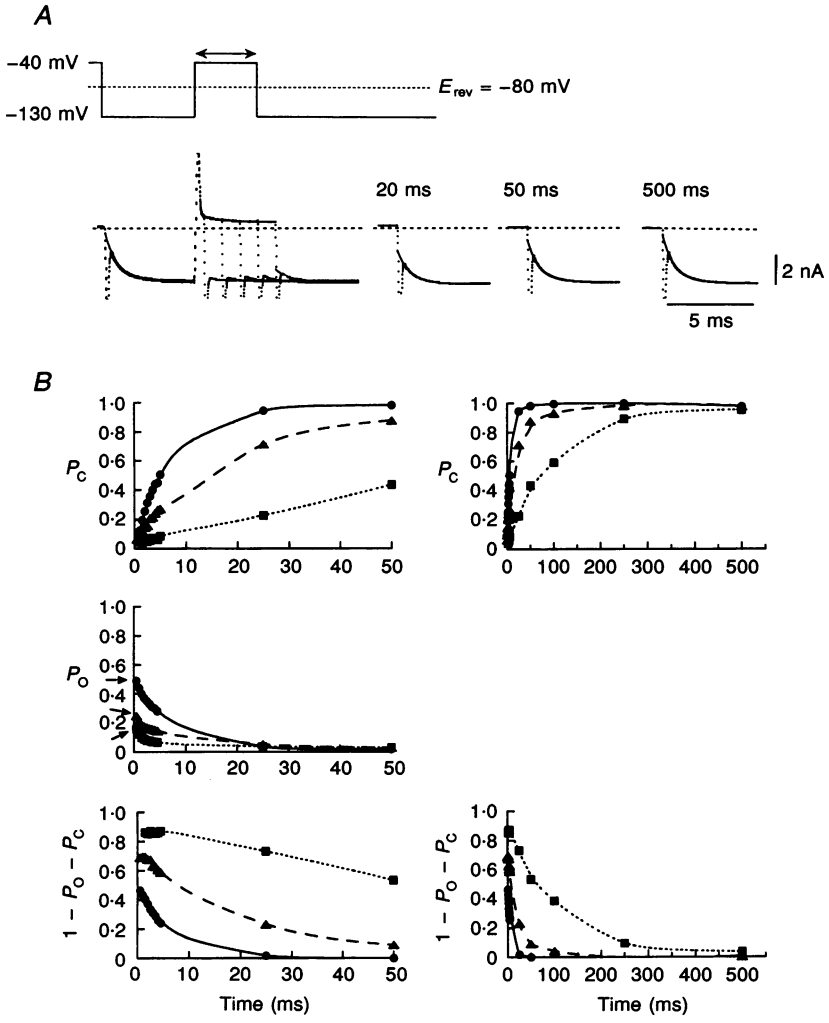

Figure 5. Non-conductive state showing instantaneous activation in the presence of divalent Put

A, envelope test performed using the Put pipette. The step pulse shown at the top was applied from the holding potential of −40 mV. Currents obtained with 0·5, 1·5, 2·5, 3·5 and 4·5 ms depolarizing pulses are superimposed, and those with longer pulses (20, 50 and 500 ms) are shown separately on the right. Single exponential curves with the time constant of 0·7 ms are fitted to inward currents. *B*, time-dependent changes of P_C (upper panel), P_O (middle panel) and the value $1 - P_O - P_C$ (lower panel) on depolarization. ●, −60 mV; ▲, −40 mV; ■, −20 mV. Data were obtained using the envelope test in *A*. For P_C, the amplitude of the time-dependent component relative to the maximum level of the inward current on repolarization is plotted against the duration of the preceding depolarization. The maximum outward current level at each depolarizing potential was estimated from the maximum chord conductance at the hyperpolarized potential, and the amplitude of the outward current normalized with this value is plotted as P_O. The value $1 - P_O - P_C$ indicates the probability of the channel being in the non-conductive state that activates virtually instantaneously on hyperpolarization. Data are interpolated by hand. Note the difference in time scale between the plots on the left and on the right.

voltage steps from a hyperpolarized level where the channels were maximally distributed in the state O. Therefore, the chronological changes of P_C, P_O and $1 - P_O - P_C$ at a certain membrane potential correspond to the time-dependent changes of those shown in Figs 5*B* and 6*B*. In the presence of either divalent cation, the voltage-dependent increase of P_C mainly caused the decrease of P_O at potentials around E_{rev}. At more positive potentials, the value $1 - P_O - P_C$ increased in a voltage-dependent manner at the expense of P_C, which was more conspicuous at the end of short depolarizations (25 ms in *A*, 20 ms in *B*). These observations imply that the blocking rate constants of Put and Mg^{2+} ($[T]\beta_T$) were larger than that of the endogenous Spm at these potentials. The time-dependent increase of P_C observed with a concomitant decrease in $1 - P_O - P_C$ can be explained if the endogenous Spm has a larger affinity ($[T]\beta_T/\alpha$) for the channel than Put or Mg^{2+} (see Discussion). In the case of Mg^{2+}, P_C increased so slowly at potentials positive to 0 mV that a large fraction of the channels were still in the Mg^{2+}-blocked state at the end of 500 ms depolarization. The efficacy of the Mg^{2+} block at the end of 500 ms voltage steps was similar to that in the native inward rectifier K^+ channel (see Fig. 5 in Ishihara *et al.* 1989).

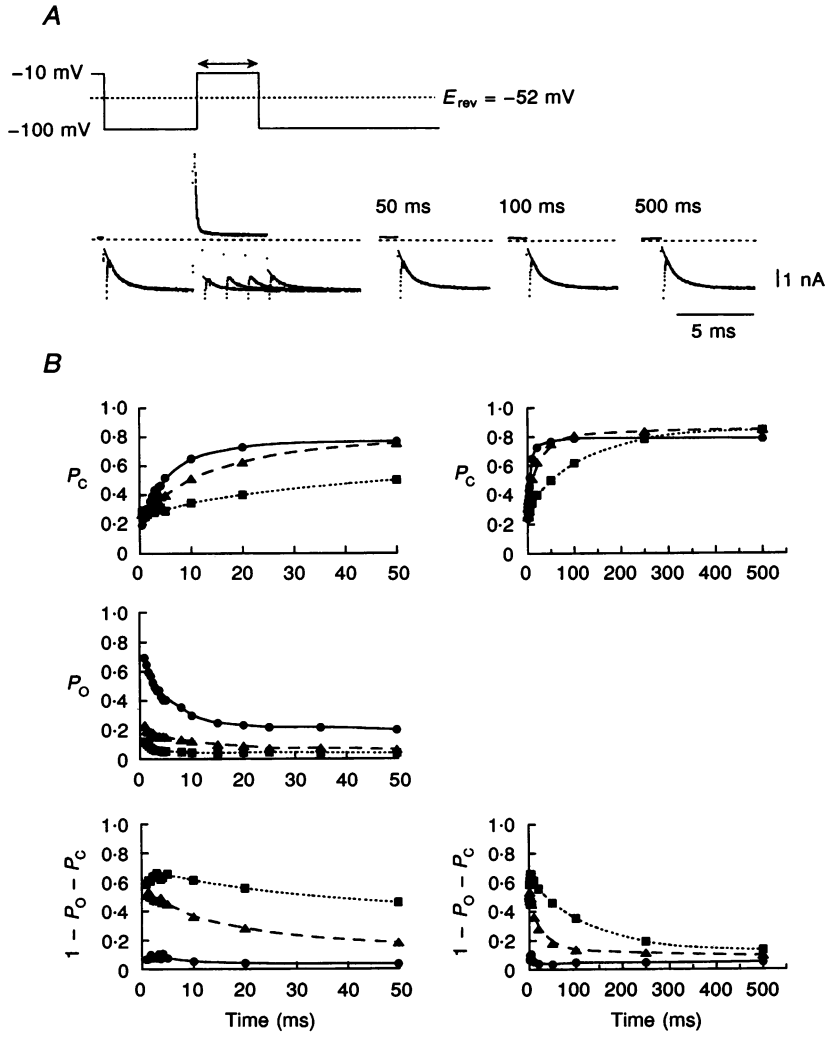

Figure 6. Mg^{2+}-blocked state on depolarization

Envelope test using the Mg^{2+} pipette. Currents were recorded at 15·4 mM K^+_o. Corresponding to the shift of E_{rev} caused by elevating $[K^+]_o$, all the membrane potentials in the step pulse were shifted in the depolarizing direction by 30 mV as compared with the pulse protocol used in Fig. 5. *A*, representative currents. Currents with 0·5, 1·5, 2·5, 3·5 and 4·5 ms depolarizing pulses are superimposed, and those with longer pulses (50, 100 and 500 ms) are shown separately on the right. *B*, time-dependent changes of P_C (upper panel), P_O (middle panel) and the value $1 - P_O - P_C$ (lower panel) on depolarization. ●, −30 mV; ▲, −10 mV; ■, 10 mV. The value $1 - P_O - P_C$ represents the probability of the channel being in the Mg^{2+}-blocked state that opens virtually instantaneously on hyperpolarization. Each value was obtained from the envelope test in *A* as described in Fig. 5*B*. Data are interpolated by hand. Note the difference in time scales between the plots on the left and on the right.

Existence of two non-conductive states in the presence of Spd

When the envelope test was performed using pipettes containing Spd, the trivalent polyamine, the amplitude of the time-dependent inward current on repolarization also increased gradually as the preceding depolarization was prolonged (Fig. 8*A*). The close inspection of the inward currents by the semilogarithmic plot revealed a double exponential time course of the time-dependent inward currents (Fig. 8*B*). Following a short depolarization, a trace of the fast time-dependent change was observed in the inward current, which could be approximated by a single exponential with the time constant of 0·28 ms (Fig. 8*Ba*, 5 ms). Following a longer depolarization, however, the time-dependent inward current was fitted by two components showing a slower component with the time constant of 0·66 ms (Fig. 8*B a*, 250 ms). The amplitude of the faster component gradually decreased, and that of the slower component increased as the depolarization was prolonged (Fig. 8*B a*, 1500 ms). This finding suggests the presence of two non-conductive states that activate with a faster (C_f) and a slower (C_s) time course. Therefore, the inward currents following various durations of depolarization were fitted by double exponential curves with the time constants of 0·28 and 0·66 ms (Fig. 8*Bb*), and the amplitude of each component relative to the maximum level of the inward current is plotted against the duration of the preceding depolarization as $P_{C,f}$ and $P_{C,s}$, respectively (Fig. 8*C*). P_O was negligible at the depolarized potentials, −60, −40 and −20 mV, and the sum of $P_{C,f}$ and $P_{C,s}$ was approximately 1·0, indicating the exclusive contribution of these two non-conductive states. During the short depolarization, the majority of the channels were in the state C_f. The time course of the transition of the channels from the state C_f to the state C_s was not significantly different at different membrane potentials in contrast to the observation obtained with Put or Mg^{2+} ($n = 6$).

Figure 8*D* shows the voltage dependence of $P_{C,s}$, $P_{C,f}$ and P_O at the end of 500 ms voltage steps applied from a hyperpolarized level using the pipette containing Spd. At each membrane potential, the sum of $P_{C,f}$ and $P_{C,s}$ agreed well

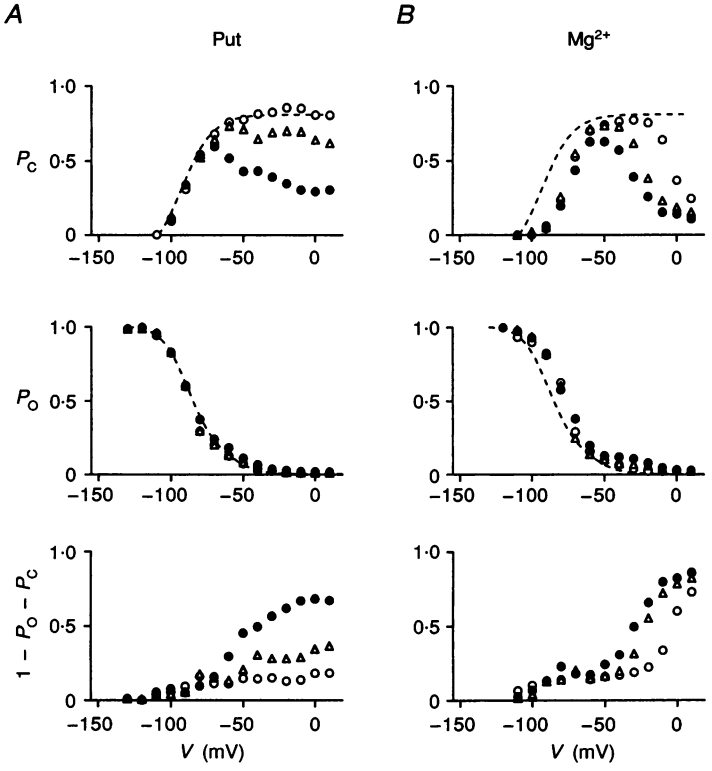

Figure 7. Voltage dependence of P_O, P_C and the value $1 - P_O - P_C$ in the presence of Put (*A*) or Mg^{2+} (*B*)

P_C (upper panel) and P_O (middle panel) were obtained at the end of various durations of voltage steps (●, 25 ms in *A*, 20 ms in *B*; △, 250 ms in *A*, 50 ms in *B*; ○, 500 ms) as described in Fig. 1*C* and *D*. The time constants of the exponentials fitted to the tail currents to obtain P_C were 0·89 ± 0·05 ms ($n = 34$) at −130 mV in *A* and 1·37 ± 0·04 ms ($n = 39$) at −120 mV in *B*. The value $1 - P_O - P_C$, representing the probability of the channel being in the non-conductive state that activates instantaneously on hyperpolarization is shown in the lower panel. Data were obtained from the experiments, which were different from those described in Figs 5 and 6. Dashed curves superimposed in P_O and P_C represent data in Fig. 1*C* and *D*.

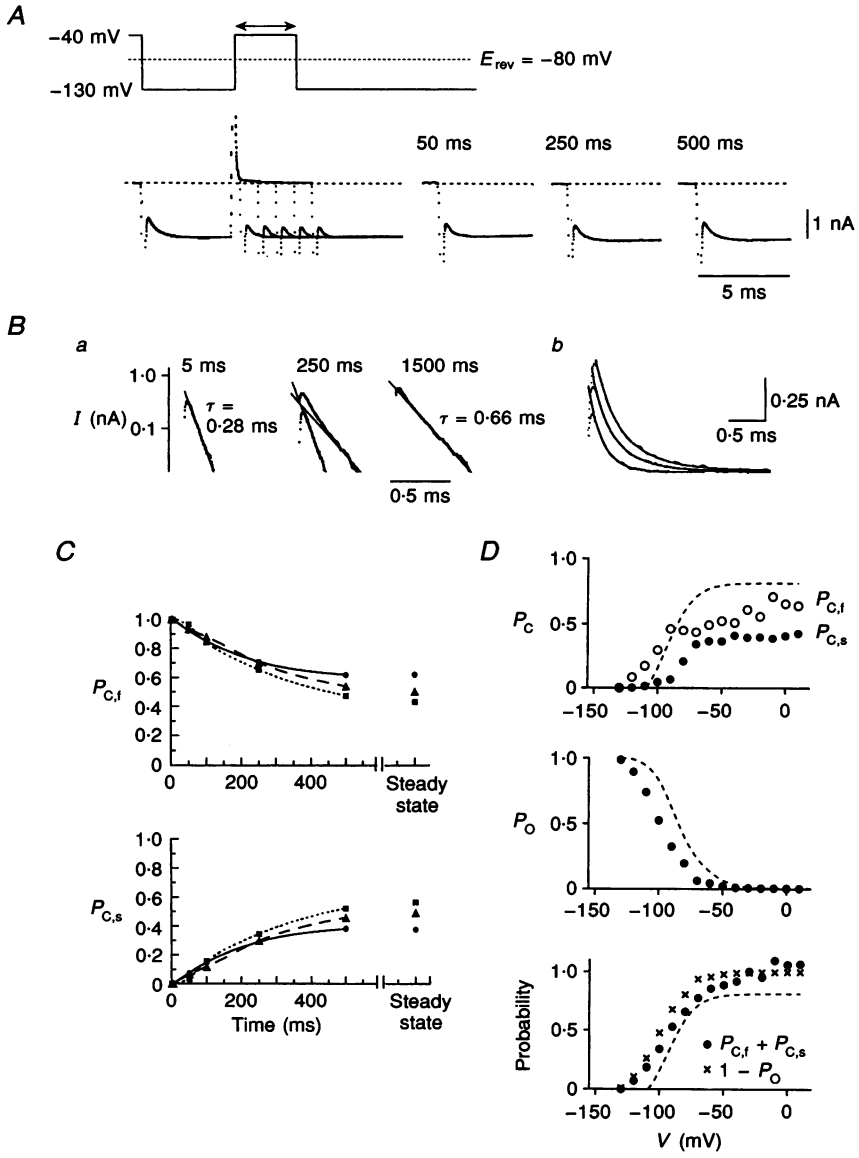

Figure 8. Effects of the trivalent cation Spd in the pipettes

A, envelope test performed using the Spd pipette. The step pulse shown at the top was applied from the holding potential of −40 mV. Currents obtained with 0·5, 1, 2, 3 and 5 ms pulses are superimposed, and those with 50, 250 and 500 ms pulses are shown on the right. *B*, fitting of the inward currents with double exponential curves. *a*, semilogarithmic plots of the inward currents on repolarization following 5, 250 and 1500 ms depolarizations. The current amplitude was measured referring to the maximum inward current level at −130 mV. The lines were fitted to the linear part of the currents by the least-squares method. At 5 and 1500 ms, the time constants were 0·28 and 0·66 ms, respectively. At 250 ms, a line was fitted to the later linear part (slow component), and the fast component was obtained as the difference between the fitted line and the original current, and is shown as the lower trace. The time constants of the slow and fast components were 0·66 and 0·28 ms, respectively. *b*, double exponential curves with the time constants of 0·28 and 0·66 ms are fitted to the inward currents. From bottom to top, the preceding depolarization was 5, 250 and 1500 ms. *C*, time-dependent changes of $P_{C,f}$ (upper panel) and $P_{C,s}$ (lower panel) on depolarization at −60 mV (●), −40 mV (▲) and −20 mV (■). The time-dependent inward currents on repolarization following various durations of depolarization were fitted by double exponential curves with time constants of 0·28 and 0·66 ms, and the amplitude of each component relative to the maximum level of the inward current is plotted against the duration of the depolarization as $P_{C,f}$ and $P_{C,s}$, respectively. Data were obtained from the envelope test in Fig. 8*A*. P_O was negligible at depolarized potentials, and the sum of $P_{C,s}$ and $P_{C,f}$ was about 1·0. *D*, voltage dependence of P_C (upper panel) and P_O (middle panel) at the end of 500 ms voltage steps applied from −130 mV. Data were obtained from a different experiment from that described in *A* and *B*. To obtain $P_{C,f}$ (○) and $P_{C,s}$ (●), tail currents following voltage steps were fitted by double exponential curves with time constants of 0·37 and 0·8 ms. In the lower panel, the sum of $P_{C,f}$ and $P_{C,s}$ (●) is compared with the value $1 - P_O$ (×). The dashed curves represent P_O and P_C in Fig. 1*C* and *D*.

with the value $1 - P_O$ (the lower panel), supporting the notion that the rectification is caused by the two non-conductive states. With Spd, the voltage dependence of P_O was shifted in the hyperpolarizing direction compared with that obtained with the Mg^{2+}-free–polyamine-free pipettes. This was mainly caused by the voltage-dependent increase of $P_{C,f}$ at membrane potentials negative to E_{rev}. $P_{C,s}$ increased at potentials positive to −100 mV showing a similar voltage dependence with that of the state C in the absence of polyamines or Mg^{2+}, and saturated at around 0·5 ($n = 3$). The appearance of the state C_f at negative potentials in the presence of Spd suggests that the state C_f is the state of the channel blocked by Spd.

Activation time course from the endogenous Spm-blocked state in the presence of Spd, Put or Mg^{2+}

Even in the presence of different blocking molecules in the pipettes, a similar time- and voltage-dependent activation of the inward currents was observed in response to hyperpolarization following a prolonged depolarization. We proposed in the previous sections that a large fraction of the channels will be blocked by the endogenous Spm after a prolonged depolarization even in the presence of Put, Mg^{2+} or Spd. Figure 9 shows the relationship between the time constant of the inward currents on hyperpolarization following a prolonged depolarization and the membrane potential in the hyperpolarization in the presence of Put, Mg^{2+} or Spd. In the case of Spd, the time constant of the slower component in the inward currents, which represents the activation from the state C_s, is plotted. The activation time constants from the state C_s were similar to those from the state C observed using the Put or the Mg^{2+} pipettes. This is compatible with the idea that the state C_s is the state of the channel blocked by the endogenous Spm. As stated above, the state C_f was inferred as the Spd-blocked state, and the unblocking of Spd was faster than that of Spm with detectable time-dependent kinetics (see also Ficker *et al.* 1994). Although the voltage dependence of the time constant was similar, the time constants were shifted in the hyperpolarizing direction, compared with those obtained using the Mg^{2+}-free–polyamine-free pipettes.

DISCUSSION

The activation kinetics of the inward rectifier K^+ channels have been described with the kinetic scheme (1) in the native channels (Hagiwara *et al.* 1976; Leech & Stanfield, 1981; Kurachi, 1985) as well as in the IRK1 channel expressed from the cloned gene (Stanfield *et al.* 1994*a*). We have proposed in this paper that the activation kinetics of the IRK1 channel reflect the blocking kinetics of the endogenous Spm. In the present study, we attempted to restore the physiological concentration of polyamines in the cultured cells, which was estimated using the activated lymphocytes and the rat liver (Watanabe *et al.* 1991). Since polyamines are deeply related to the cell growth (Pegg, 1988), they may be less abundant in terminally differentiated cells, such as neuronal cells and cardiac myocytes that express the inward rectifier K^+ channels. When we added tetravalent Spm in the pipettes, the inward rectification of the currents occurred at more negative potentials, and the changes in the activation

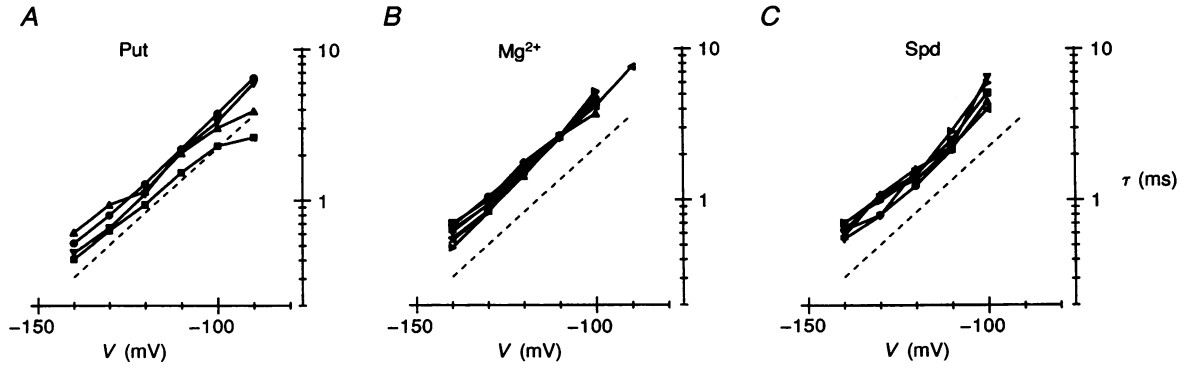

Figure 9. Activation time constant from the endogenous Spm-blocked state in the presence of Put, Mg^{2+} or Spd

A–C, time constants of the inward currents elicited on hyperpolarization from the holding potential of −10 mV. Data were obtained using the pipettes containing Put (*A*), Mg^{2+} (*B*) or Spd (*C*). In *A* and *B*, time constants were obtained by fitting single exponential curves to the currents. In *C*, double exponential curves were fitted to the inward currents when the capacitive transients decayed fast enough to acknowledge the fast component, and the time constants of the slower component, which we proposed as the activation time constant from the state C_s, are plotted. The time constants of the fast component (the activation from the state C_f) were 0·39 ± 0·10 ms ($n = 4$), 0·50 ± 0·2 ms ($n = 5$) and 0·75 ms (means, $n = 3$) at −130, −120 and −110 mV, respectively. Data were recorded at least 15 min after starting the experiments. The number of the experiments is 4, 7 and 6 in *A*, *B* and *C*, respectively. The dashed lines represent data in Fig. 1*B*.

kinetics indicated a 10–20 times increase in the 'closing' rate constant β, implying that the non-conductive state C represents the Spm-blocked state of the channel. By adding the other cations, Spd, Put, or Mg^{2+} in the pipettes, different non-conductive states that show faster activation time courses appeared besides the state C. Therefore we concluded that Spm is the molecule generating the 'intrinsic gating' of the channel (Ishihara *et al.* 1989; Silver & DeCoursey, 1990). The divalent Put block that caused the instantaneous current change on hyperpolarization contributed to the instantaneous rectification of the current on large depolarizations like the Mg^{2+} block (Ishihara *et al.* 1989; Silver & DeCoursey, 1990). Our conclusion is in line with the notion that the rectification of the inward rectifier K^+ channel results from the voltage-dependent block of the channel by internal molecules (Hagiwara & Takahashi, 1974; Hille & Schwarz, 1978). Since the blocking effect is restricted by the concentration of the permeant K^+, however, the 'K^+ activation mechanism' may also exist to regulate the availability of the block (Ciani *et al.* 1978; Carmeliet, 1982; Pennefather *et al.* 1992; Pennefather & DeCoursey, 1994).

In the present study, we also showed that the apparent slow-down of the deactivation time course, which was caused by Put or Mg^{2+} in the pipettes, is concurrent with the slow decrease of the Put- or the Mg^{2+}-blocked channels during depolarization (Figs 5 and 6). Even in the presence of Put or Mg^{2+}, the block of the endogenous Spm mainly produced the inward rectification of the currents around E_{rev} (Fig. 7), indicating that the affinity of Spm for the channel was larger than that of Put or Mg^{2+} at this potential range. We consider that the extremely slow increase of the endogenous Spm-blocked state at large depolarizations reflects the time course of the replacement of the blocking molecule from Put or Mg^{2+} to the endogenous Spm that has a larger affinity with the channel. By simulating the same phenomenon using the computer model, we showed that the redistribution of the channels from the Mg^{2+}-blocked state to the 'closed state' of the native channel through the open state occurs during depolarization (Ishihara *et al.* 1989). When there are two non-conductive states that can be taken by the channels on depolarization, channels will be first distributed more to the state showing a larger transition rate constant ($[T]\beta_T$, in scheme (2)). If the other non-conductive state has a larger affinity ($[T]\beta_T/\alpha$) due to the small unblocking rate constant α, however, channels will be redistributed further to this non-conductive state. At the single channel level, the Spm and the Spd block show much longer dwell times than that of the Put block in the IRK1 channel (Ficker *et al.* 1994) or than that of the Mg^{2+} block in the native channel (Matsuda, 1988), indicating a small unblocking rate α that often leads to the high affinity blocking of molecules (Hille, 1992). The Mg^{2+} block showing a large unblocking rate paradoxically increases P_O (Matsuda, 1988). The redistribution of the channels from such a blocked state to the state showing a small unblocking rate will result in a slow decay of outward currents during depolarization (Figs 5 and 6). Thus, the voltage dependence of P_O in the presence of Mg^{2+} showed a hump in the relationship at potentials between −50 and −10 mV, which disappeared when the Mg^{2+} block diminished (Fig. 7*B*).

In the presence of Spd, Put or Mg^{2+} in the pipettes, the time constant of the activation phase reflecting the unblocking of the endogenous Spm was shifted in the hyperpolarizing direction by about 10–15 mV (Fig. 9). The equivalent slowing of the activation was shown by Fakler *et al.* (1995) with 1 mM Mg^{2+} using the cell-free patch, whereas Stanfield *et al.* (1994*b*) reported that 10 mM Mg^{2+} causes a similar shift under the whole-cell clamp. Since we consider that Spm does not block the channel while the channel is plugged by Put or Mg^{2+}, the blocking effects of Spd, Put or Mg^{2+} are unlikely to be involved in the shift of the time constant. Even if the Spm-blocked state can be 'blocked' further by the molecules at the different site at the channel orifice (Shioya, Matsuda & Noma, 1993), it is difficult to produce the shift of the time constant. Therefore, we speculate that the shift of the time constant was caused by the decrease in the transmembrane potential through screening the fixed negative charges on the membrane surface or at the channel orifice. The shift of the rate constant α in the hyperpolarizing direction observed by adding Spm to the pipettes (Fig. 3*E*) may be the common effect caused by the increased amount of cations at the inner surface of the membrane. The subsequent decrease in the surface concentration of permeant K^+ will shift the relationship in the opposite direction.

Polyamines are the strong bases protonated at physiological pH. Judging from the virtually instantaneous unblocking of Put and Mg^{2+} (Figs 5 and 6), and the faster unblocking of Spd compared with that of Spm (Fig. 8), the order of the unblocking rate constant at hyperpolarized potentials appeared to be Put $\approx Mg^{2+} >$ Spd > Spm, corresponding inversely to the number of the charges in each molecule. Therefore, it is possible that the organic cations, polyamines, block the channel through their binding to the channel by means of the electrostatic force. It has been shown that the single negatively charged amino acid in the putative second transmembrane region of the IRK1 channel is responsible for the long closed time of the Spm/Spd block at depolarized potentials (Ficker *et al.* 1994), and for the time-dependent activation of the inward current on hyperpolarization (Stanfield *et al.* 1994*b*; Wible *et al.* 1994; Ficker *et al.* 1994; Fakler *et al.* 1994; Fakler *et al.* 1995). If the IRK1 channel is a tetramer (Kubo *et al.* 1993), the matching of the number of positive charges in the Spm molecule with that of the negative charges lining the channel pore (Stanfield *et al.* 1994*b*) may be structurally important for the high affinity of Spm.

CARMELIET, E. (1982). Induction and removal of inward-going rectification in sheep cardiac Purkinje fibres. *Journal of Physiology* **327**, 285–308.

CIANI, S., KRASNE, S., MIYAZAKI, S. & HAGIWARA, S. (1978). A model for anomalous rectification: electrochemical-potential-dependent gating of membrane channels. *Journal of Membrane Biology* **44**, 103–134.

COHEN, I. S., DIFRANCESCO, D., MULRINE, N. K. & PENNEFATHER, P. (1989). Internal and external K^+ help gate the inward rectifier. *Biophysical Journal* **55**, 197–202.

FABIATO, A. & FABIATO, F. (1979). Calculator programs for computing the composition of the solutions containing multiple metals and ligands used for experiments in skinned muscle cells. *Journal de Physiologie* **75**, 463–505.

FAKLER, B., BRANDLE, U., BOND, C., GLOWATZKI, E., KONIG, C., ADELMAN, J. P., ZENNER, H.-P. & RUPPERSBERG, J. P. (1994). A structural determinant of differential sensitivity of cloned inward rectifier K^+ channels to intracellular spermine. *FEBS Letters* **356**, 199–203.

FAKLER, B., BRANDLE, U., GLOWATZKI, E., WEIDEMANN, S., ZENNER, H.-P. & RUPPERSBERG, J. P. (1995). Strong voltage-dependent inward rectification of inward rectifier K^+ channels is caused by intracellular spermine. *Cell* **80**, 149–154.

FICKER, E., TAGLIALATELA, M., WIBLE, B. A., HENLEY, C. M. & BROWN, A. M. (1994). Spermine and spermidine as gating molecules for inward rectifier K^+ channels. *Science* **266**, 1068–1072.

HAGIWARA, S., MIYAZAKI, S. & ROSENTHAL, N. P. (1976). Potassium current and the effect of cesium on this current during anomalous rectification of the egg cell membrane of a starfish. *Journal of General Physiology* **67**, 621–638.

HAGIWARA, S. & TAKAHASHI, K. (1974). The anomalous rectification and cation selectivity of the membrane of a starfish egg cell. *Journal of Membrane Biology* **18**, 61–80.

HILLE, B. (1992). Mechanisms of block. In *Ionic Channels of Excitable Membranes*, 2nd edn, pp. 390–422. Sinauer Associates Inc., Sunderland, MA, USA.

HILLE, B. & SCHWARZ, W. (1978). Potassium channels as multi-ion single-file pores. *Journal of General Physiology* **72**, 409–442.

HORIE, M., IRISAWA, H. & NOMA, A. (1987). Voltage-dependent magnesium block of adenosine-triphosphate-sensitive potassium channel in guinea-pig ventricular cells. *Journal of Physiology* **387**, 251–272.

ISHIHARA, K. & HIRAOKA, M. (1994). Gating mechanism of the cloned inward rectifier potassium channel from mouse heart. *Journal of Membrane Biology* **142**, 55–64.

ISHIHARA, K., MITSUIYE, T., NOMA, A. & TAKANO, M. (1989). The Mg^{2+} block and intrinsic gating underlying inward rectification of the K^+ current in guinea-pig cardiac myocytes. *Journal of Physiology* **419**, 297–320.

KUBO, Y. (1994). Towards the elucidation of the structural–functional relationship of inward rectifying K^+ channel family. *Neuroscience Research* **21**, 109–117.

KUBO, Y., BALDWIN, T. J., JAN, Y. N. & JAN, L. Y. (1993). Primary structure and functional expression of a mouse inward rectifier potassium channel. *Nature* **362**, 127–133.

KURACHI, Y. (1985). Voltage-dependent activation of the inward-rectifier potassium channel in the ventricular cell membrane of guinea-pig heart. *Journal of Physiology* **366**, 365–385.

LEECH, C. A. & STANFIELD, P. R. (1981). Inward rectification in frog skeletal muscle fibres and its dependence on membrane potential and external potassium. *Journal of Physiology* **319**, 295–309.

LOPATIN, A. N., MAKHINA, E. N. & NICHOLS, C. G. (1994). Potassium channel block by cytoplasmic polyamines as the mechanism of intrinsic rectification. *Nature* **372**, 366–369.

MAKHINA, E. N., KELLY, A. J., LOPATIN, A. N., MERCER, R. W. & NICHOLS, C. G. (1994). Cloning and expression of a novel human brain inward rectifier potassium channel. *Journal of Biological Chemistry* **269**, 20468–20474.

MATSUDA, H. (1988). Open-state substructure of inwardly rectifying potassium channels revealed by magnesium block in guinea-pig heart cells. *Journal of Physiology* **397**, 237–258.

MATSUDA, H. (1993). Effects of internal and external Na^+ ions on inwardly rectifying K^+ channels in guinea-pig ventricular cells. *Journal of Physiology* **460**, 311–326.

MATSUDA, H. & CRUZ, J. D. S. (1993). Voltage-dependent block by internal Ca^{2+} ions of inwardly rectifying K^+ channels in guinea-pig ventricular cells. *Journal of Physiology* **470**, 295–311.

MATSUDA, H., SAIGUSA, A. & IRISAWA, H. (1987). Ohmic conductance through the inwardly rectifying K channel and blocking by internal Mg^{2+}. *Nature* **325**, 156–159.

MAZZANTI, M. & DIFRANCESCO, D. (1989). Intracellular Ca modulates K-inward rectification in cardiac myocytes. *Pflügers Archiv* **413**, 322–324.

NIWA, H., YAMAMURA, K. & MIYAZAKI, J. (1991). Efficient selection for high-expression transfectants by a novel eukaryotic vector. *Gene* **108**, 193–200.

PEGG, A. E. (1988). Polyamine metabolism and its importance in neoplastic growth and as a target for chemotherapy. *Cancer Research* **48**, 759–774.

PENNEFATHER, P., OLIVA, C. & MULRINE, N. (1992). Origin of the potassium and voltage dependence of the cardiac inwardly rectifying K-current (I_{K1}). *Biophysical Journal* **61**, 448–462.

PENNEFATHER, P. S. & DECOURSEY, T. E. (1994). A scheme to account for the effects of Rb^+ and K^+ on inward rectifier K channels of bovine artery endothelial cells. *Journal of General Physiology* **103**, 549–581.

PERIER, F., RADEKE, C. M. & VANDENBERG, C. A. (1994). Primary structure and characterization of a small-conductance inwardly rectifying potassium channel from human hippocampus. *Proceedings of the National Academy of Sciences of the USA* **91**, 6240–6244.

SHIOYA, T., MATSUDA, H. & NOMA, A. (1993). Fast and slow blockades of the inward-rectifier K^+ channel by external divalent cations in guinea-pig cardiac myocytes. *Pflügers Archiv* **422**, 427–435.

SILVER, M. R. & DECOURSEY, T. E. (1990). Intrinsic gating of inward rectifier in bovine pulmonary artery endothelial cells in the presence or absence of internal Mg^{2+}. *Journal of General Physiology* **96**, 109–133.

STANFIELD, P. R., DAVIES, N. W., SHELTON, P. A., KHAN, I. A., BRAMMAR, W. J., STANDEN, N. B. & CONLEY, E. C. (1994*a*). The intrinsic gating of inward rectifier K^+ channels expressed from the murine IRK1 gene depends on voltage, K^+ and Mg^{2+}. *Journal of Physiology* **475**, 1–7.

STANFIELD, P. R., DAVIES, N. W., SHELTON, P. A., SUTCLIFFE, M. J., KHAN, I. A., BRAMMAR, W. J. & CONLEY, E. C. (1994*b*). A single aspartate residue is involved in both intrinsic gating and blockage by Mg^{2+} of the inward rectifier, IRK1. *Journal of Physiology* **478**, 1–6.

VANDENBERG, C. A. (1987). Inward rectification of a potassium channel in cardiac ventricular cells depends on internal magnesium ions. *Proceedings of the National Academy of Sciences of the USA* **84**, 2560–2564.

WATANABE, S.-I., KUSAMA-EGUCHI, K., KOBAYASHI, H. & IGARASHI, K. (1991). Estimation of polyamine binding to macromolecules and ATP in bovine lymphocytes and rat liver. *Journal of Biological Chemistry* **266**, 20803–20809.

WIBLE, B. A., TAGLIALATELA, M., FICKER, E. & BROWN, A. M. (1994). Gating of inwardly rectifying K^+ channels localized to a single negatively charged residue. *Nature* **371**, 246–249.

YANAGI, Y., HU, H.-L., SEYA, T. & YOSHIKURA, H. (1994). Measles virus infects mouse fibroblast cell lines, but its multiplication is severely restricted in the absence of CD46. *Archives of Virology* **138**, 39–53.

Acknowledgements

We thank Drs L. Y. Jan and Y. Kubo for providing us with the IRK1 gene, Dr J. Miyazaki for providing us with the pCXN2 vector, and Dr Y. Yanagi for his suggestions. We also thank Drs Y. Hara and Y. Ikawa for providing us with facilities, and Dr T. Ehara for reading the manuscript. This work was supported by the Grant-in-Aid for Scientific Research on Priority Areas of Channel–Transporter Correlation from the Ministry of Education, Science and Culture of Japan. K.I. also thanks Casio Science Promotion Foundation for its support.

Received 28 April 1995; accepted 11 September 1995.